

Electron Temperature Measurement Using Electron Cyclotron Emission on LHD

NAGAYAMA Yoshio, INAGAKI Shigeru, ITO Yasuhiko, KAWAHATA Kazuo,
MORISAKI Tomohiro, KOMORI Akio, NARIHARA Kazumichi, OHYABU Nobuyoshi,
SAKAKIBARA Satoru, TANAKA Kenji and LHD Experimental Group
National Institute for Fusion Science, Toki, 509-5292, Japan

(Received: 21 December 2001 / Accepted: 2 August 2002)

Abstract

The ECE diagnostics have been developed in LHD. Two antenna sets are installed in the outboard side of LHD. The ECE detected by the perpendicular antenna has a linear polarization, which is determined at the plasma boundary, but the ECE emitted in the tangential direction is not linearly polarized. The ECE system is calibrated with a hot (800 K) radiation source and a high gain amplifier, which are calibrated with a cold (77 K) radiation source. The ECE temperature agrees with the Thomson scattering measurement and the diamagnetism in LHD. The ECE is employed to observe the magnetic island, which is generated with a local island divertor field. The island width approaches to the vacuum width as the plasma beta increases, unexpectedly.

Keywords:

electron cyclotron emission (ECE), large helical device (LHD), local island divertor (LID), polarization, electron temperature, magnetic island

1. Introduction

The electron cyclotron emission (ECE) diagnostics is a well established technique for the continuous measurement of the electron temperature profile in tokamaks. In helical systems, however, very few experiments have been reported on ECE measurements. Fundamental differences between helical systems and tokamaks in terms of ECE measurement are the polarization and the magnetic field profile. In helical systems, the magnetic field profile is peaked and the angle of field line varies from -30 to $+30$ degrees, while the magnetic field is monotonic and the angle of field line varies very small in tokamaks. The emissivity of ECE at the plasma center, where the magnetic field is peak, is smaller than the black body radiation. Along the sight line tangential to the plasma, however, the peak of the magnetic field shifts to inboard side. So, the electron

temperature in the plasma center may be measured using ECE. In LHD an ECE antenna of the tangential sight line is newly installed in the outboard side. This paper reports the recent progress of the ECE measurement in LHD, and also reports the first experimental result obtained by using the tangential antenna.

The intensity calibration is an important issue in the ECE diagnostics. In order to obtain the electron temperature, the ECE intensity has to be calibrated by a black body radiation source with the known temperature. This paper reports the calibration using a hot radiation source in LHD. In order to reduce noise, the signal has to be integrated in long period. Since the signal from our hot (800 K) source is three times stronger than that from the usual cold (77 K) source, the signal to noise ratio increases by factor three with the

Corresponding author's e-mail: nagayama@nifs.ac.jp

same integration time. In order to examine the reliability, the ECE temperature is compared with the electron temperature obtained by the other apparatus, such as Thomson scattering and the diamagnetism, in this paper.

The variation of temperature profile can be distinguished easily using ECE diagnostics because of low noise. This feature is adequate to investigate magnetic island structure. Recently, the physics of magnetic island attracts attention [5]. This paper presents the first ECE measurement of the magnetic island structure, which is produced by using the local island divertor (LID) field.

2. ECE System and Electron Temperature Measurement

Schematic diagram of ECE measurement system in the outboard side is shown in Fig. 1. The detail of the conventional ECE system in LHD is presented in refs. [1-3]. We also present experimental results using the ECE detection system in the inboard side of LHD in this conference [4]. In order to reduce the transmission loss, the ECE system fully uses the corrugated waveguide system in LHD. A tangential antenna is newly installed in LHD. The calculated magnetic field along the sight line is shown in Fig. 2. The corresponding normalized plasma radius ρ is also plotted in Fig. 2. In this case, the tangential sight line is shifted vertically, this line does not pass the right center of plasma, unfortunately. Since the magnetic field is peaked at the plasma center, the ECE from the plasma center cannot be detected on the perpendicular sight line. On the other hand, since the

magnetic field is still increased at the plasma center, it is expected that the ECE from the plasma center can be detected on the tangential sight line. The perpendicular antenna and the tangential antenna can be switched shot by shot using a switch in the corrugated waveguide system.

The ECE system with the fast scanning Michelson interferometer (Michelson) is calibrated using a hot (800 K) radiation source in order to obtain the electron temperature. In order to increase the calibration signal, a polarizer, which is to be set at 45 degrees in the plasma experiment, is set at 0 degrees, and a high-gain active low-pass filter is additionally used in order to reduce digitally sampled error (so called bit-noise). The hot source and the other additionally used components in the calibration process are also calibrated with a liquid nitrogen cooled (77 K) radiation source. The calibration signal of one million scans is integrated. The radiometer data is calibrated to the Michelson temperature.

The electron temperature obtained by ECE is compared with other diagnostics, such as the Thomson scattering and the diamagnetism. In Fig. 3, the electron temperature profile measured using ECE and Thomson scattering in cases of low density and high density. Electron temperature measured with ECE and Thomson scattering agrees well in wide range of density. In Fig. 4, the ECE temperature is compared with the diamagnetic temperature in various plasmas. Here, the diamagnetic temperature, T_{dia} is defined as:

$$W_p = 3 \int n_e(\rho) T_e(\rho) dV.$$

Here, the T_e and n_e profiles are assumed typical profiles

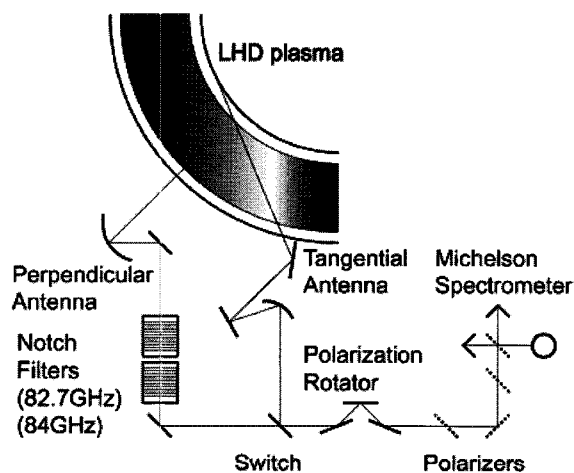


Fig. 1 Schematic diagram of ECE measurement system in the outboard side in LHD.

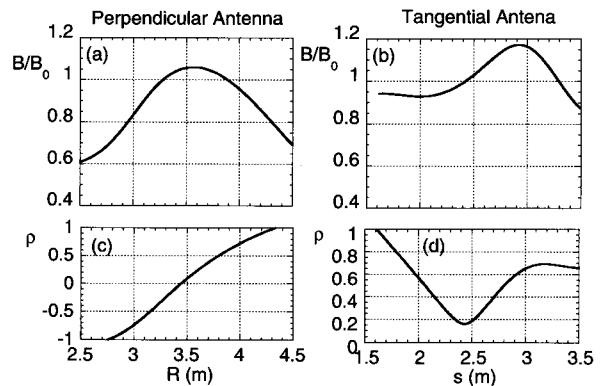


Fig. 2 (a) Magnetic field on the sight line of the perpendicular antenna. (b) Magnetic field on the sight line of the tangential antenna. (c) Normalized plasma radius on the sight line of the perpendicular antenna. (d) Normalized plasma radius on the sight line of the tangential antenna.

in LHD, as follows:

$T_i(\rho) = T_e(\rho) = T_{dia} (1 - \rho^2)$, $n_e(\rho) = n_{e0} (1 - \rho^8)$. Figure 4 shows that the ECE temperature is consistent with the diamagnetic temperature, basically. In low-density plasmas when the ECE is optically thick, however, the ECE temperature is saturated while the diamagnetic temperature increases. This is very interesting phenomena.

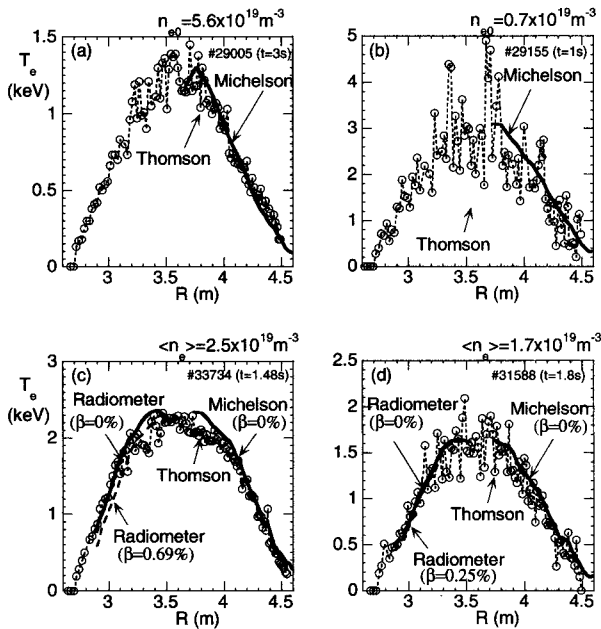


Fig. 3 Electron temperature profile measured with ECE and Thomson scattering in (a) high density case, (b) low density case, (c) high beta case ($\beta=0.69\%$), (d) low beta case ($\beta=0.25\%$).

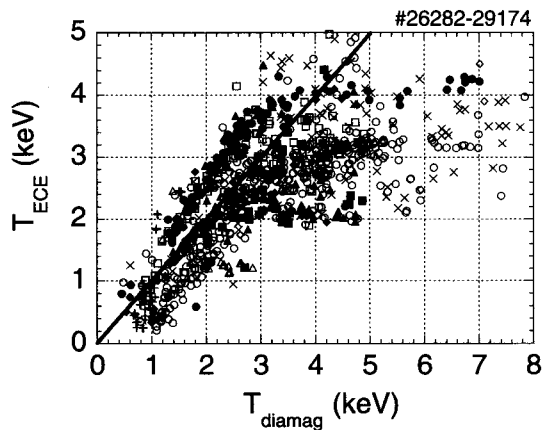


Fig. 4 Electron temperature obtained by ECE and the diamagnetic measurements. Different marks indicate shots in different days. Closed marks indicate $R_{ax}=3.5$ m, open marks indicate $R_{ax}=3.6$ m, and cross marks indicate $R_{ax}=3.75$ m.

These results indicate that the obtained electron temperature by these diagnostics is reliable in moderate density LHD plasmas.

3. Polarization

Figure 5 shows polarization of ECE detected by the perpendicular and the tangential antennas. The magnetic field is 2.8T and the line averaged electron density is $1.4 \times 10^{19} \text{ m}^{-3}$. ECE signals of 148 GHz and 127 GHz have a peak at 25 degrees and bottom is at 70 degrees on the perpendicular sight line, as shown in Fig. 5(a). Note the ECE signal detected by the tangential antenna is not calibrated. ECE signal of 75 GHz has a peak at 70 degrees and bottom is at 25 degrees. The difference is 45 degrees. The rotation angle of the ECE polarization is double of the polarization rotator angle. So, the difference of the polarization angle is 90 degrees. When the microwave source (Gunn-oscillator) is set at the angle perpendicular to the field line of the last closed flux surface, the peak is at 25 degrees. Therefore, the 148 GHz and 127 GHz have the same polarization angle as the X-mode on the last closed flux surface, and the 70 GHz has the same polarization angle as the O-mode.

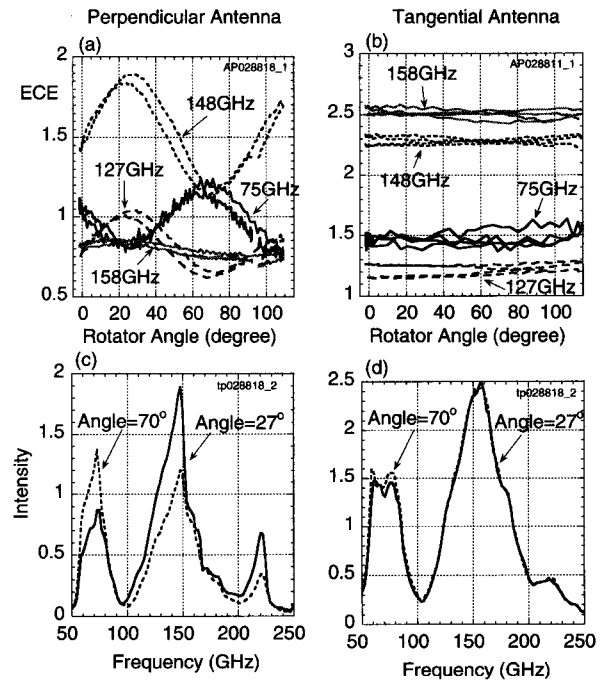


Fig. 5 (a) Polarization of ECE detected by the perpendicular antenna. (b) Polarization of ECE detected by the tangential antenna. (c) Spectrum of ECE detected by the perpendicular antenna. (d) Spectrum of ECE detected by the tangential antenna.

The different frequency corresponds to the different radiation place, where the field angle is different. So, the polarization of ECE is determined at the plasma boundary. The spectrum has peaks at 74 GHz and at 148 GHz, which corresponds to the fundamental O-mode and the second harmonic X-mode in case of perpendicular antenna.

Figure 5(c) shows the spectrum of ECE detected by the perpendicular antenna, when the polarization is at X-mode (27 degrees) and at the O-mode (70 degrees). The fundamental O-mode, of which frequency is between 50 GHz and 75 GHz, is stronger than the fundamental X-mode. The second-harmonic X-mode, of which frequency is between 100 GHz and 150 GHz, is stronger than the second-harmonic O-mode. ECE between 75 and 100 GHz and between 150 GHz and 200 GHz is not polarized. These ECE are generated near the coil where the magnetic field is higher than the plasma center. They have to be scattered at the wall, and lose the polarization when enter the antenna.

Figure 5(b) show the polarization of ECE detected by the tangential antenna. The tangentially emitted ECE is not linearly polarized in this experiment. This is consistent with the theoretical prediction that the tangentially emitted ECE has a circular polarization. Figure 5(d) show the spectrum of the tangentially emitted ECE. As we expect in the introduction of this paper, the spectrum of the second harmonics is symmetric with the center frequency of 155 GHz. The higher frequency than 155 GHz may come from the high field region, which is on the sight line of the tangential antenna. Interestingly, the spectrum less than 100 GHz detected by the tangential antenna are quite different from that detected by the perpendicular antenna. The fundamental ECE spectrum have two peaks, one at 62 GHz another at 78 GHz. The peak at 78 GHz may correspond to the ECE from the center of plasma. However, the peak at 62 GHz is rather mysterious. Tangentially emitted ECE has not been well understood because theoretical and experimental works are very limited.

4. Magnetic Island

Observation of magnetic island structure is one of useful applications of ECE measurement, since the relative error is small in ECE measurements. Figure 6(a) shows the calculated magnetic island structure generated by the LID field in vacuum. Figure 6(b) shows the electron temperature profiles of LHD plasmas with and without LID field. The electron temperature gradient in

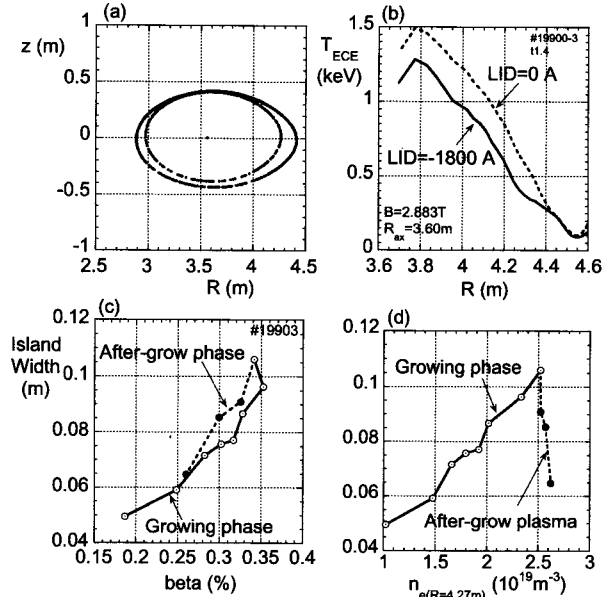


Fig. 6 (a) Calculated magnetic island structure. (b) Electron temperature profile measured using ECE (Michelson spectrometer) with and without LID field. (c) Trajectory of shot 19903 on the plane of island width vs. beta. (d) Trajectory on the plane of island width vs. electron density.

the region between $R = 4.27$ m and $R = 4.43$ m is less than that in the other places. This region is close to the vacuum magnetic island structure in Fig. 6(a). The island region is not flat in the temperature profile, but the electron temperature profile in the inner region surrounded by the island is reduced due to the island. The temperature profile is shifted as much as the vacuum island width. Now, we define the experimental island width as the radial displacement in the electron temperature profile. Figure 6(c) shows trajectory of the island width on the beta during a single discharge. The magnetic island grows as the beta increases during the growing phase, and it shrinks as the beta decreases in the after-grow phase. This trajectory indicates that the island width depends on the beta. Figure 6(d) shows trajectory of the island width on the electron density. In the growing phase the island grows as the density increases. In the after-grow phase, however, the density is constant while the island width decreases. The island width does not look to depend on the electron density but it depends on the beta. Most interesting point is that as the beta increases the magnetic island approaches to the width in vacuum, in which the beta should be zero.

5. Conclusion

The ECE diagnostics have been developed in LHD. Two antenna sets are installed in the outboard side of LHD. The ECE detected by the perpendicular antenna has a linear polarization, which is determined at the plasma boundary, but the ECE emitted in the tangential direction is has not linear polarization. The electron temperature is calibrated with a hot (800 K) radiation source and a high gain amplifier, which are calibrated with a cold (77 K) radiation source. The ECE temperature agrees with the Thomson scattering measurement and the diamagnetism in moderate density plasmas in LHD. The ECE is used to observe the magnetic island, which is generated with a LID field. The island width approaches to the vacuum width as the

plasma beta increases, unexpectedly. It requires further investigation to understand these phenomena.

Refereneces

- [1] Y. Nagayama, K. Kawahata, A. England *et al.*, *Rev. Sci. Instrum* **70**, 1034 (1999).
- [2] Y. Nagayama, K. Kawahata, S. Inagaki, H. Sasao *et al.*, *Fusion Eng. Des.* **53**, 201 (2001).
- [3] P.C. de Vries, K. Kawahata, Y. Nagayama *et al.*, *Phys. Plasmas* **7**, 3707 (2000).
- [4] S. Inagaki, Y. Nagayama *et al.*, *presented in this conference*.
- [5] K. Narihara, K.Y. Watanabe, I. Yamada *et al.*, *Phys. Rev. Lett.* **87**, 24 (2001).